Engineered Science
DOI: https://dx.doi.org/10.30919/es2029

Iterative Synthesis of Initial Kinematic Chains with Rotational Pairs Based on Stepwise Minimization of Geometric Deviations

Gulbarshyn Smailova,[1] Algazy Zhauyt,[2,*] Kuanysh Alipbayev,[2] Nazgul Kaliyeva,[2] Yerlan Yeleukulov,[2] Alisher Aden,[2] Alfiya Atalykova[3] and Nurgul Kurmahgaliyeva[2]

Abstract

This paper addresses the problem of synthesizing four-link initial kinematic chains with rotational pairs for designing flat lever mechanisms with specified motion laws of the input and output links. The proposed method formulates the synthesis problem as an optimization process involving three moving planes Q, $Q1$ and $Q2$. Each plane performs distinct motions: Q is fixed, $Q1$ rotates around a point A, and $Q2$ undergoes plane-parallel motion. The goal is to determine the optimal position of point $A \in Q$, $B \in Q1$ and $C \in Q2$ such that the distance between points B and C remains nearly constant across multiple configurations. The synthesis problem is reduced to a sequence of linear systems of equations corresponding to three iterative minimization stages: Determining the fixed-point A and the radius R for given points B and C; Determining the point B and radius R for a given point C; Determining the point C and radius R for a given point B. The algorithm uses a hierarchical optimization process to iteratively refine the positions of A, B, and C until convergence is achieved. The convergence criteria are defined by the small changes in the positions of these points and the radius R between iterations. The proposed method avoids solving a highly nonlinear system directly by decomposing the problem into simpler linear systems, ensuring computational efficiency and robustness. The solution provides the desired positions of the points, forming an open kinematic chain $ABCD$ with three degrees of freedom. The approach is applicable to the synthesis of complex planar mechanisms with unrestricted parameters, making it a valuable tool for mechanism design.

Keywords: Kinematic synthesis; Initial kinematic chain; Approximate kinematic geometry; Objective function minimization; System of linear equations.
Received: 20 September 2025; Revised: 08 December 2025; Accepted: 19 January 2026
Article type: Research article.

1. Introduction

1.1 Research background

The synthesis of planar lever mechanisms is a fundamental problem in mechanical system design, especially for applications requiring precise motion transfer between input and output links. Engineering practice frequently demands mechanisms capable of guiding rigid bodies through prescribed position sets while ensuring reliable kinematic performance. To address these requirements, initial kinematic chains (IKCs) serve as foundational structural units for constructing complex flat mechanisms. These chains allow the designer to describe the relative motion of two moving bodies with respect to a fixed base and provide a systematic foundation for mechanism synthesis.

1.2 Current research status and existing problems

Existing approaches to mechanism synthesis have largely developed along two directions: algebraic approximation methods and methods based on approximate kinematic geometry. Although these approaches have contributed significantly to classical linkage design, they exhibit several limitations when applied to modern engineering tasks. Numerical methods often require partial parameter specification, rely heavily on good initial guesses, and do not guarantee convergence to a global optimum. Classical geometric approaches, while elegant, struggle when extended to high-class mechanisms or hybrid kinematic pairs. Furthermore, many current synthesis methods do not provide

[1]*Department of Mechanical Engineering, Satbayev University, Almaty, 050013, Kazakhstan*
[2]*Department of Aerospace and Electronic Engineering, Almaty University of Power Engineering and Telecommunications named after Gumarbek Daukeyev, Almaty, 050013, Kazakhstan*
[3]*Department of Automation and Control, Almaty University of Power Engineering and Telecommunications named after Gumarbek Daukeyev, Almaty, 050013, Kazakhstan*
[*]*Email*: zhauyt@aues.kz (A. Zhauyt)

a complete workflow—from structural definition to dimensional synthesis—limiting their applicability in automated design environments.

1.3 Research highlights

To overcome these limitations, this work develops a unified numerical–analytical method for the structural and kinematic synthesis of planar mechanisms based on initial kinematic chains and their modifications. The proposed framework extends the theory of approximate kinematic geometry to encompass four-link IKCs with rotational and translational pairs, enabling simultaneous determination of structure and dimensions. A stepwise minimization algorithm is introduced to compute all unknown parameters analytically or semi-analytically while ensuring geometric consistency across multiple prescribed positions. The method supports full automation, is computationally efficient for implementation on standard personal computers, and enables the design of both conventional and high-class mechanisms from a unified foundation.

2. Materials and methods

Let there be given N discrete positions of two planes, denoted as Q_1 and Q_2, which represent sections of two rigid bodies. Their positions relative to a fixed reference plane Q are specified as follows: plane Q_1 is defined by coordinates (X_A, Y_A) and a rotation angle φ_i about point A in Fig. 1a, where $i = 1, \dots, N$; plane Q_2 is defined by coordinates (X_{Di}, Y_{Di}) and a rotation angle ψ_i about point D in Fig. 1b and Eq. (1), for the same $i = 1, \dots, N$:

$$Q_1(X_A, Y_A, \varphi_i),\ Q_2(X_{Di}, Y_{Di}, \psi_i),\ i = 1, \dots, N \qquad (1)$$

To formalize the motions: A rectangular coordinate system OXY is rigidly attached to the fixed plane Q. The moving planes Q_1 and Q_2 each carry their own coordinate systems: A_{xy}, fixed in Q_1; $D_i x_i' y_i'$, fixed in Q_2 for each position i. In this setup: plane Q_1 undergoes pure rotational motion about the fixed-point A; plane Q_2 executes a general plane-parallel motion,[1] governed by the trajectory of point D and rotation ψ. The aim is to synthesize a kinematic chain-typically a four-bar linkage-capable of guiding these two bodies through the given set of positions with high precision, ideally minimizing deviations using methods of approximate synthesis. Where X_A, Y_A - is the fixed-point A on the base plane Q; x_B, y_B - is the coordinates of hinge B on Q_1; x_C, y_C - is the coordinates of hinge C on Q_2; X_{Di}, Y_{Di} - is the path (trajectory) of point D on Q_2; φ_i - is the rotation angle of Q_1 in position i; ψ_i - is the rotation angle of Q_2 in position i; a, c - is the coefficients of straight line equation (*e.g.* for translational guidance); R - length of connecting link. Research manuscripts reporting large datasets that are deposited in a publicly available database should specify where the data have been deposited and provide the relevant accession numbers. If the accession numbers have not yet been obtained at the time of submission, please state that they will be provided during review. They must be provided prior to publication. To achieve coordinated motion of the two moving planes Q_1 and Q_2, geometric connections must be established between them. These connections can be implemented in two principal ways, leading to different types of four-link kinematic chains: 1. Kinematic chain with a two-hinged link. In this case, a rigid link with rotational (revolute) pairs is used to directly connect the two moving planes: The resulting mechanism is a closed four-link kinematic chain $ABCD$ in Fig. 1c, consisting entirely of rotational joints and having three degrees of freedom;[2] The configuration is illustrated schematically in Fig. 1d; The task is to determine the positions of three key points: $A \in Q$ - a fixed hinge on the stationary plane; $B \in Q_1$ - a hinge point on the first moving plane; $C \in Q_2$ a hinge point on the second moving plane. These points must be chosen such that the mechanism ensures the specified laws of motion (*i.e.*, prescribed positions and orientations of Q_1 and Q_2) across all N configurations. 2. Kinematic chains with a link group (open chains). Alternatively, coordination can be achieved using a link group that combines rotational and translational pairs: The guide link is attached to one of the moving planes, and the stone link (slider or connecting link) is pivotally attached to the other. This configuration yields two open variants of the four-link chain: Variant ACD: rotational pair at A, translational pair along line CD; Variant ABD: rotational pair at A in Fig. 1e and Fig. 1f, translational pair along line BD. Both variants retain three degrees of freedom,[2] but they differ in how motion is transferred between Q_1 and Q_2. In this approach, synthesis requires: Determining the coefficients (slope and intercept) of the guiding line equation, along which translational motion occurs. Specifying the position of the hinge: $B \in Q_1$ in the ABD configuration; $C \in Q_2$ in the ACD configuration. Identifying the fixed hinge point $A \in Q$ on the stationary plane. This Fig. 2 presents the geometric configurations of initial four-link kinematic chains with rotational pairs formed by connecting two moving planes Q_1 and Q_2 through a fixed base plane Q. The subfigures illustrate the different problem formulations and corresponding parameter groupings used in the synthesis algorithm: Full configuration of the four-bar chain ABCD, showing the fixed base point $A \in Q$, and moving points $B \in Q_1$, $C \in Q_2$, and the constant inter-hinge distance R. Intermediate configurations for each minimization step: Solving for A while B and C are fixed; Solving for B while A and C are fixed; Solving for C while A and B are fixed. Reduced configurations corresponding to boundary cases (*e.g.*, fixing one point or setting coordinates to zero) for simplifying the linear systems.[3,4] Each subfigure corresponds to a stage in the stepwise synthesis algorithm, supporting convergence to a locally optimal mechanism by solving linearized subsystems (as described in systems Eq. (17)).

This Fig. 2a, Fig. 2b, Fig. 2c, Fig. 2d, Fig. 2e and Fig. 2f presents geometric configurations for synthesizing kinematic chains of type ACD and AD, where the connection between

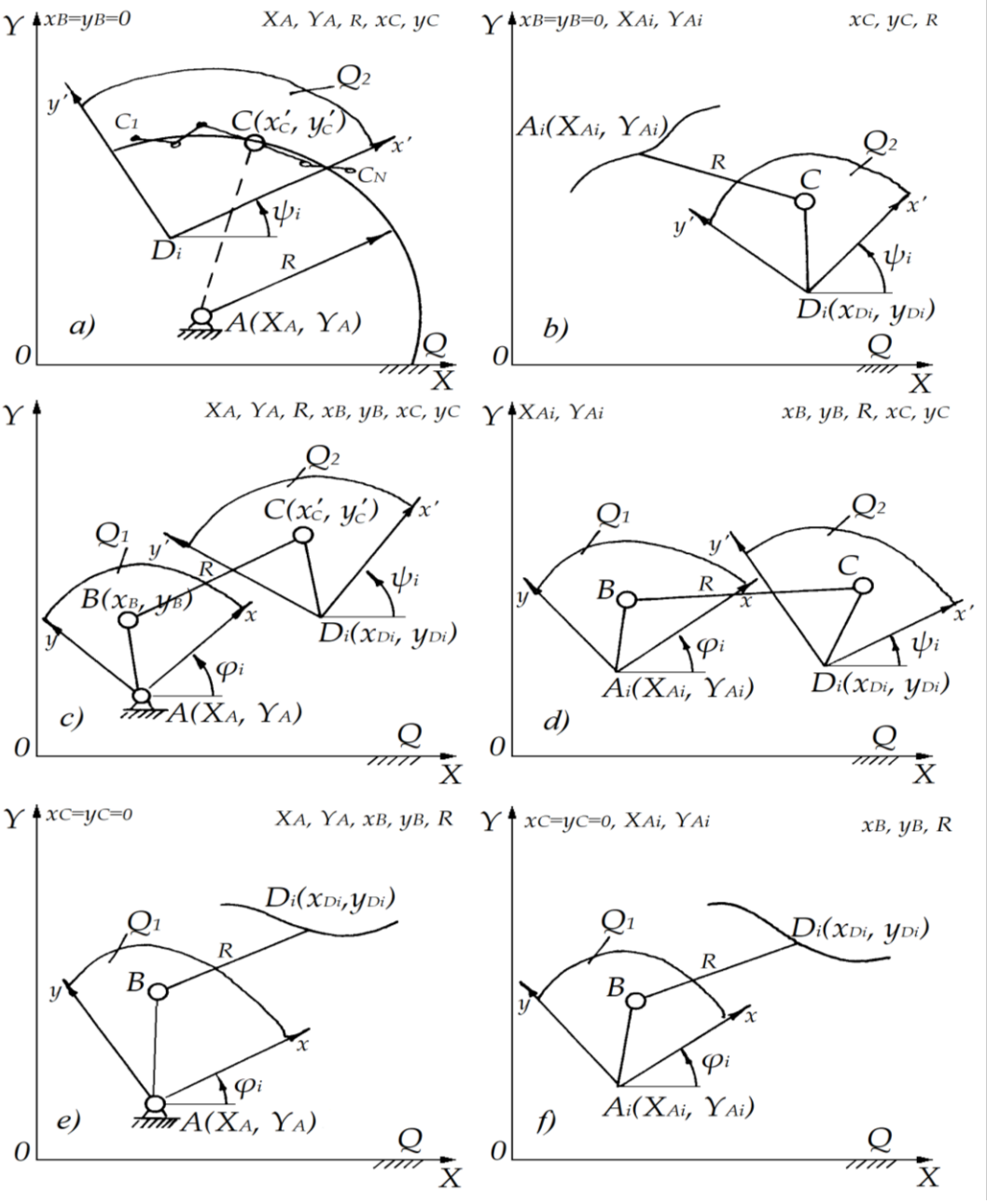


Fig. 1: Configurations of synthesized initial kinematic chains: closed four-bar link chain (*ABCD*) and open variants (*ACD*, *ABD*).

the moving planes Q_1 and Q_2 is implemented using one rotational and one translational pair.[5] The aim is to constrain the motion of one point (typically on Q_2) to follow an approximately linear path relative to another plane. Initial configurations with known base point $A \in Q$ and a point $C \in Q_2$ moving along a path defined implicitly by the guiding line. Simplified geometric construction of the motion constraint imposed on point C. Line equation $ax + by + c = 0$ is imposed on point C trajectory relative to plane Q_1. Plane-parallel motion and angular orientation of plane Q_2 shown relative to base Q.

Reduced cases where specific coordinates are zeroed $x_C = y_C = 0$ for simplification in solving the associated linear systems.[6] These configurations correspond to problem formulations using expressions for $\Delta_{qi}^{(3)}$, and systems Eq. (24) and Eq. (23), leading to identification of optimal line parameters a, c, and base point coordinates. This Fig. 2c supports the second synthesis problem discussed in the paper, where the objective is to determine optimal hinge placement and line constraints to guide motion coordination through translational pair synthesis.[7]

This Fig. 3a, Fig. 3b, Fig. 3c, Fig. 3d, Fig. 3e and Fig. 3f depicts the geometric arrangements for the synthesis of *ABD* and *AD* kinematic chains, where the moving planes Q_1 and Q_2 are connected through one fixed base plane Q using a combination of rotational and translational pairs. In this formulation, the trajectory of point $B \in Q_1$ is constrained relative to plane Q_2 via an approximate straight-line path,[8] while point $A \in Q$ serves as the rotation base. Initial geometric setup where the straight-line guiding point B is implicitly

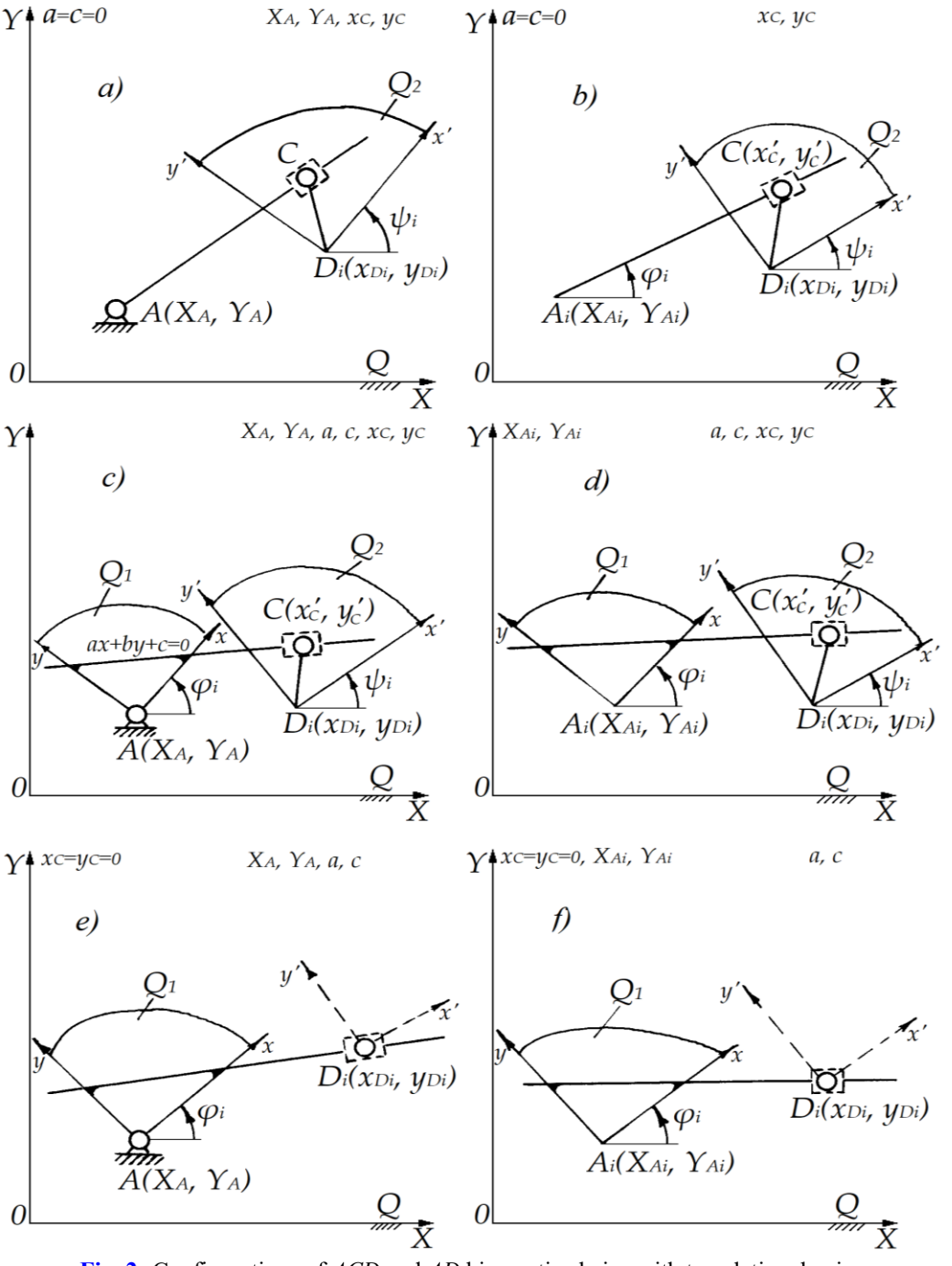


Fig. 2: Configurations of *ACD* and *AD* kinematic chains with translational pairs.

defined through transformations relative to Q_2. Local coordinate system and motion vector orientation of point $D_i \in Q_2$.[9]

Explicit formulation of the constraint line $ax + by + c = 0$, through which point B trajectory is minimized. Graphical construction of synthesis problems to determine the optimal hinge coordinates and line parameters on Q_1 and Q_2. Reduced boundary cases for solving simplified systems by setting $x_B = y_B = 0$, enabling direct solution of line parameters a, c for motion planning in the translational domain. These configurations support the third synthesis problem of the study,[10] where the objective is to determine optimal placement of the base point $A \in Q$, line coefficients a, c, and hinge location $B \in Q_1$ such that the movement is constrained according to translational behavior. Fig. 3c corresponds to solving systems such as Eq. (24) and Eq. (23) with appropriate linearization.[11]

3. Synthesis of initial kinematic chain with rotation pairs (ABCD Chain)

To determine the linear dimensions of the closed four-link initial kinematic chain *ABCD* is shown in Fig. 1c, we formulate the synthesis task as a geometric optimization problem. The aim is to ensure that the distance between two

moving points - one on each of the mobile planes Q_1 and Q_2 - remains approximately constant across multiple specified positions.[5,12]

Problem 1. Synthesis of *ABCD* initial kinematic chain with rotation pairs.

$A(X_A, Y_A) \in Q$ – on the stationary base plane;

$B(x_B, y_B) \in Q_1$ - fixed in the local coordinate system Eq. (2) of the first moving plane;

$C(x'_C, y'_C) \in Q_2$ - fixed in the local coordinate system Eq. (3) of the second moving plane.

Such that the distance between B and C remains close to a constant R for all given finite relative positions $i = 1,2,\dots,N$ of the planes Q_1 and Q_2.

For each position i, we are given:

Plane Q_1: defined by rotation angle φ_i around point A;

Plane Q_2: defined by rotation angle ψ_i and displacement X_{Di}, Y_{Di} of point D.

The coordinates of points B and C at each position i, relative to the global system OXY Eq. (4), are obtained using homogeneous transformation matrices.

Point B in Q_1 (rotation about A):

$$\begin{bmatrix} x_{Bi} \\ y_{Bi} \\ 1 \end{bmatrix} = \begin{bmatrix} cos\varphi_i & -sin\varphi_i & X_A \\ sin\varphi_i & cos\varphi_i & Y_A \\ 0 & 0 & 1 \end{bmatrix} \begin{bmatrix} x_B \\ y_B \\ 1 \end{bmatrix} \quad (2)$$

Point C in Q_2 (undergoing planar motion):

$$\begin{bmatrix} x_{Ci} \\ y_{Ci} \\ 1 \end{bmatrix} = \begin{bmatrix} cos\psi_i & -sin\psi_i & X_{Di} \\ sin\psi_i & cos\psi_i & Y_{Di} \\ 0 & 0 & 1 \end{bmatrix} \begin{bmatrix} x'_C \\ y'_C \\ 1 \end{bmatrix} \quad (3)$$

For each position i, the constraint is:

$$(x_{Ci} - x_{Bi})^2 + (y_{Ci} - y_{Bi})^2 \approx R^2 \quad (4)$$

The deviation from this constraint across all N positions is minimized using an objective function, typically the sum of squared deviations:

$$S = \sum_{i=1}^{N} [(x_{Ci} - x_{Bi})^2 + (y_{Ci} - y_{Bi})^2 - R^2]^2$$

Unknown parameters to determine (7 total):

X_A, Y_A – are the coordinates of the base point $A \in Q$;

x_B, y_B – are the coordinates of the hinge point $B \in Q_1$ in its local frame;

x'_C, y'_C – are the coordinates of the hinge point $C \in Q_2$ in its local frame;

R – is the approximate link length between points B and C;

Problem 2. Synthesis of *ACD* initial kinematic chain with rotational and translational pairs.

This problem concerns the synthesis of an open initial kinematic chain[13,14] of the form *ACD* is shown in Fig. 2c, in which one link endpoint is constrained to move along a straight line (a prismatic pair), and the other endpoint is pivotally connected to the second moving body.

A base hinge point $A(X_A, Y_A) \in Q$;

A straight line $ax + by + c = 0$ - fixed in the coordinate system of plane Q_1;

A point $C(x'_C, y'_C) \in Q_2$ – defined in the local frame of Q_2.

Such that the trajectory of point C (from plane Q_2) approaches the desired straight line (defined in Q_1) as closely as possible across *N* given motion positions.

This task defines the synthesis of an open initial kinematic chain *ACD* with mixed kinematic pairs:

A is a rotational pair between the fixed base and plane Q_1;

C is a point constrained to slide along a line (*i.e.*, a prismatic pair) defined in the frame of Q_1.

This is appropriate for mechanisms such as guide-link couplers or line-follower linkages, where one endpoint traces a line and the opposite pivot is free to rotate.

For each position i, point $C \in Q_2$ (in its local coordinates x'_C, y'_C) is transformed into the global frame using a homogeneous transformation:

$$\begin{bmatrix} x_{Ci} \\ y_{Ci} \\ 1 \end{bmatrix} = \begin{bmatrix} cos\psi_i & -sin\psi_i & X_{Di} \\ sin\psi_i & cos\psi_i & Y_{Di} \\ 0 & 0 & 1 \end{bmatrix} \begin{bmatrix} x'_C \\ y'_C \\ 1 \end{bmatrix}$$

We define the desired guidelines on plane Q_1 in its local coordinates by $ax + by + c = 0$. To express this line in the global frame OXY, we apply the inverse transformation of plane Q_1 motion for each position i. The condition that transformed point Ci lies approximately on the transformed line yields:

$$\begin{aligned} a[(x_{Ci} - X_A)cos\varphi_i + (y_{Ci} - Y_A)sin\varphi_i] \\ + b[-(x_{Ci} - X_A)sin\varphi_i \\ + (y_{Ci} - Y_A)cos\varphi_i] + c \approx 0 \end{aligned}$$

This expression represents the signed distance from point Ci to the moving guideline (transformed to the global system), and we seek to minimize the sum of squared deviations from this line across all positions:

$$S = \sum_{i=1}^{N} [a \cdot \xi_i + b \cdot \eta_i - c]^2$$

$$\begin{aligned} \xi_i = (x_{Ci} - X_A)cos\varphi_i + (y_{Ci} - Y_A)sin\varphi_i; \eta_i = \\ -(x_{Ci} - X_A)sin\varphi_i + (y_{Ci} - Y_A)cos\varphi_i \end{aligned} \quad (5)$$

Unknown parameters (7 total):

X_A, Y_A – is the position of hinge A on base plane Q;

a, b, c – are the coefficients of the line equation (defined in Q_1 frame);

x'_C, y'_C – are the local coordinates Eq. (5) of point C on plane Q_2.

Problem 3. Synthesis of ABD initial kinematic chain with translational pairs.

This problem addresses the design of an open initial kinematic chain *ABD* is shown in Fig. 3c, in which the motion of a point $B \in Q_1$ is constrained to approximate a straight-line trajectory defined in the local coordinate system Eq. (24) of the second moving plane Q_2.

A fixed hinge point $A(X_A, Y_A) \in Q$;

A moving point $B(x_B, y_B) \in Q_1$ - defined in the local

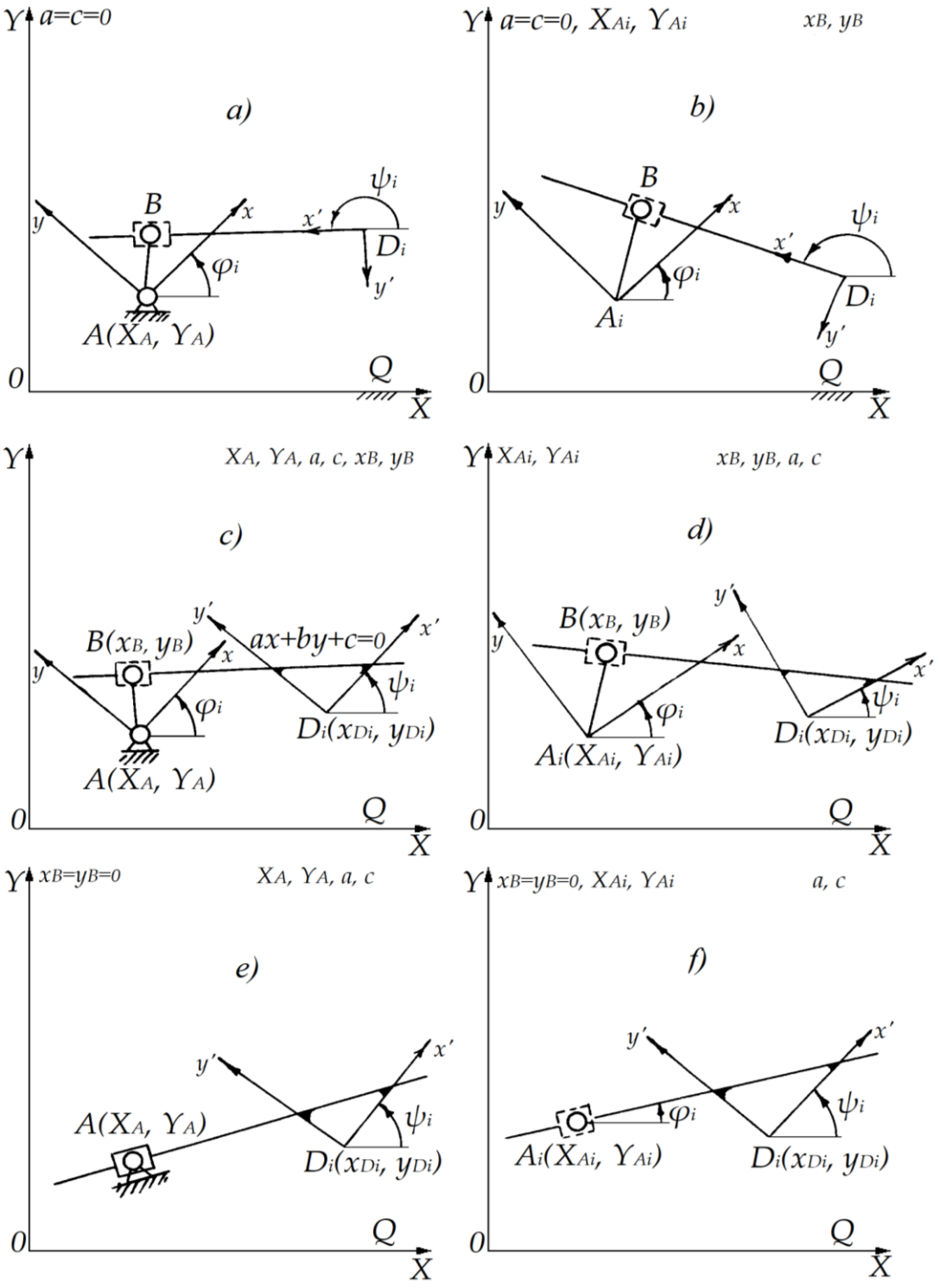


Fig. 3: Configurations of *ABD* and *AD* kinematic chains with translational pairs.

coordinate frame of Q_1;

A line $ax + by + c = 0$ defined in the coordinates system Eq. (6) of plane Q_2.

$$ax + by + c = 0 \tag{6}$$

Such that the trajectory of point B, when transformed through Q_1 motion relative to the global base and observed from Q_2, remains as close as possible to this specified straight line during the entire motion cycle.

This is the synthesis of an *ABD*-type open initial kinematic chain with mixed kinematic pairs:

The point $A \in Q$ acts as a revolute joint to the input plane Q_1;

The point $B \in Q_1$ is constrained to follow a line on plane Q_2, corresponding to a prismatic pair.

Such configurations are frequently found in planar guiding mechanisms,[15] single-stroke cams, and reciprocating systems where a point from the input side slides along a

path defined by the output body.

The position of point $B \in Q_1$, given in local coordinates x_B,y_B, transforms to the global OXY frame as:

$$\begin{bmatrix} x_{Bi} \\ y_{Bi} \\ 1 \end{bmatrix} = \begin{bmatrix} cos\varphi_i & -sin\varphi_i & X_A \\ sin\varphi_i & cos\varphi_i & Y_A \\ 0 & 0 & 1 \end{bmatrix} \begin{bmatrix} x_B \\ y_B \\ 1 \end{bmatrix}$$

The straight line in Q_2, defined by $ax + by + c = 0$ in local coordinates, transforms into the global frame for each position i of Q_2, using:

$$\begin{aligned} a[(x_{Bi} - X_{Di})cos\psi_i + (y_{Bi} - Y_{Di})sin\psi] \\ + b[-(x_{Bi} - X_{Di})sin\psi_i \\ + (y_{Bi} - Y_{Di})cos\psi_i] + c \approx 0 \end{aligned}$$

This expression computes the signed distance from point Bi global position to the line defined on Q_2 at position i.

To ensure closeness of point B to the desired trajectory across all N positions, we minimize the squared sum of line deviations:

$$S = \sum_{i=1}^{N} [a \cdot \xi_i + b \cdot \eta_i - c]^2$$

$$\begin{aligned} \xi_i = (x_{Bi} - X_{Di})cos\psi_i + (y_{Bi} - Y_{Di})sin\psi; \eta_i = \\ -(x_{Bi} - X_{Di})sin\psi_i + (y_{Bi} - Y_{Di})cos\psi_i \end{aligned} \quad (7)$$

Unknown (7 total):
X_A, Y_A – are the location Eq. (7) of the fixed base pivot $A \in Q$;
x_B, y_B – are the position of the moving point $B \in Q_1$;
a, b, c – are the coefficients defining the straight-line constraint in Q_2.

This synthesis problem ensures that the motion of a point $B \in Q_1$, when projected onto plane Q_2, approximates a known line.[6,16] Together with Problem 2, it completes the strategy for designing initial kinematic chains that involve one translational constraint. Both Problem 2 (ACD) and Problem 3 (ABD) fall under the broader class of synthesis problems with translational pairs, where the guiding geometry is defined in a moving frame and the mechanism must conform to hybrid (rotational and prismatic) link constraints.[17]

4. Weighted differences for synthesis with rotational pairs

4.1 First form of the weighted difference (Optimizing Over X_A, Y_A, R)

We want the length between the moving points B_i and C_i to be approximately constant:

$$\begin{aligned} \Delta_{qi} = |B_iC_i|^2 - R^2 = (x_{Ci} - x_{Bi})^2 + (y_{Ci} - y_{Bi})^2 \\ - R^2 \end{aligned} \quad (8)$$

This expression is a function of the seven unknown parameters: X_A, Y_A, x_B, y_B, x'_C, y'_C, R. To calculate Δ_{qi}, we first need to compute x_{Bi}, y_{Bi} and x_{Ci}, y_{Ci} the positions of points B and C in the global coordinate system Eq. (8) and Eq. (9).

We define:

$$\begin{aligned} \Delta_{qi}^{(1)} = (X_{Ai} - X_A)^2 + (Y_{Ai} - Y_A)^2 - R^2 \text{ for } i = \\ 1, \dots, N \end{aligned} \quad (9)$$

where X_{Ai}, Y_{Ai} is the composite transformed difference vector from B_i to C_i, expressed as:

$$\begin{aligned} \begin{bmatrix} X_{Ai} \\ Y_{Ai} \\ 1 \end{bmatrix} = -\begin{bmatrix} cos\varphi_i & -sin\varphi_i & 0 \\ sin\varphi_i & cos\varphi_i & 0 \\ 0 & 0 & 1 \end{bmatrix} \begin{bmatrix} x_B \\ y_B \\ 1 \end{bmatrix} + \\ \begin{bmatrix} cos\psi_i & -sin\psi_i & X_{Di} \\ sin\psi_i & cos\psi_i & Y_{Di} \\ 0 & 0 & 1 \end{bmatrix} \begin{bmatrix} x'_C \\ y'_C \\ 1 \end{bmatrix} \end{aligned} \quad (10)$$

This gives the relative vector $\overrightarrow{C_i}$ - $\overrightarrow{B_i}$ mapped into global coordinates Eq. (10), allowing you to separate the search for optimal (X_A, Y_A, R) while treating the rest as known or intermediate.

We break the total error Δ_{qi} into different function forms (likely for simplification in optimization):

Form 1: $\Delta_{qi}^{(1)} = f(X_A, Y_A, R)$

Form 2: $\Delta_{qi}^{(2)} = f(x_B, y_B, R)$

Form 3: $\Delta_{qi}^{(3)} = f(x'_C, y'_C, R)$

Each form treats a different group of parameters as variables while holding the rest fixed or transformed into intermediate quantities. This can help in iterative numerical solutions, where we minimize over subsets of parameters alternately.[18]

We define the sum of squared Eq. (11) weighted deviations for N given positions:

You define the sum of squared weighted deviations for N given positions:

$$\begin{aligned} S^{(1)} = \sum_{i=1}^{N} \left(\Delta_{qi}^{(1)}\right)^2 = \sum_{i=1}^{N} [(X_{Ai} - X_A)^2 + (Y_{Ai} - \\ Y_A)^2 - R^2]^2 \end{aligned} \quad (11)$$

where X_{Ai} , Y_{Ai} are functions of known data and the transformation matrices; X_A, Y_A, R are unknowns to be found.

To minimize S Eq. (12), take partial derivatives with respect to each unknown and set them to zero:

$$\frac{\partial S}{\partial X_A} = 0; \quad \frac{\partial S}{\partial Y_A} = 0; \quad \frac{\partial S}{\partial R} = 0 \quad (12)$$

From your derivation Eq. (13), using the chain rule and applying the structure of $\Delta_{qi}^{(1)}$, we arrive at:

$$\begin{aligned} \sum_{i=1}^{N} \Delta_{qi}^{(1)} (X_{Ai} - X_A) = 0 \\ \sum_{i=1}^{N} \Delta_{qi}^{(1)} (Y_{Ai} - Y_A) = 0 \\ \sum_{i=1}^{N} \Delta_{qi}^{(1)} R = 0 \end{aligned} \quad (13)$$

To avoid the meaningless solution $R = 0$, assume $R \neq 0$. Then:

$$\sum_{i=1}^{N} \Delta_{qi}^{(1)} = 0 \tag{14}$$

This simplifies the previous system Eq. (14). Substituting this result back in, the system becomes:

$$\begin{gathered} \sum_{i=1}^{N} \Delta_{qi}^{(1)} X_{Ai} = 0 \\ \sum_{i=1}^{N} \Delta_{qi}^{(1)} Y_{Ai} = 0 \\ \sum_{i=1}^{N} \Delta_{qi}^{(1)} = 0 \end{gathered} \tag{15}$$

These are your final minimization conditions.

Step-by-step substitution from Eq. (9) into system Eq. (15):

$$\begin{gathered} \sum_{i=1}^{N}[2X_{Ai}^2 X_A + 2X_{Ai}Y_{Ai}Y_A + X_{Ai}(R^2 - X_A^2 - Y_A^2)] = \sum_{i=1}^{N}(X_{Ai}^2 + Y_{Ai}^2)X_{Ai} \\ \sum_{i=1}^{N}[2X_{Ai}Y_{Ai}X_A + 2Y_{Ai}^2 Y_{Ai} + Y_{Ai}(R^2 - X_A^2 - Y_A^2)] = \sum_{i=1}^{N}(X_{Ai}^2 + Y_{Ai}^2)Y_{Ai} \\ \sum_{i=1}^{N}[2X_{Ai}X_A + 2Y_{Ai}Y_A + (R^2 - X_A^2 - Y_A^2)] = \sum_{i=1}^{N}(X_{Ai}^2 + Y_{Ai}^2) \end{gathered} \tag{16}$$

We perform a powerful transformation that simplifies the nonlinear system Eq. (16) into a linear system of equations by introducing a new variable:

$$H_1 = \frac{1}{2}(R^2 - X_A^2 - Y_A^2)$$

This substitution transforms the previously nonlinear problem into a linear least-squares formulation, enabling direct matrix solution.[19] Let's now clearly walk through our transformation and express everything in compact, structured matrix Eq. (17) form.

Let's write the system you obtained in matrix form:

$$\begin{bmatrix} \sum X_{Ai}^2 & \sum X_{Ai}Y_{Ai} & \sum X_{Ai} \\ \sum X_{Ai}Y_{Ai} & \sum Y_{Ai}^2 & \sum Y_{Ai} \\ \sum X_{Ai} & \sum Y_{Ai} & N \end{bmatrix} \begin{bmatrix} X_A \\ Y_A \\ H_1 \end{bmatrix} = \frac{1}{2} \begin{bmatrix} \sum R_{Ai}^2 X_{Ai} \\ \sum R_{Ai}^2 Y_{Ai} \\ \sum R_{Ai}^2 \end{bmatrix} \tag{17}$$

where $R_{Ai}^2 = X_{Ai}^2 + Y_{Ai}^2$ This system is linear and can be solved using any standard method (Gaussian elimination, LU decomposition, or matrix inversion Eq. (18)), provided $R \neq 0$, which guarantees that the Jacobian of the transformation is non-zero:

$$\left\| \frac{\partial(X_A, Y_A, H_1)}{\partial(X_A, Y_A, R)} \right\| = R$$

As we stated in the first form:

$$(X_A, Y_A, H_1) = \frac{1}{D_1}(D_{XA}, D_{YA}, D_{H1}), \text{ for } D_1 \neq 0 \tag{18}$$

Then, from:

$$R = \sqrt{X_A^2 + Y_A^2 + 2H_1}$$

This remains valid and analytically elegant, assuming non-degeneracy of the determinant.

4.2 Second form of the weighted difference (Optimizing Over x_B, y_B, R)

In this second formulation Eq. (19), the goal is to express the squared deviation $\Delta_{qi}^{(2)}$ in terms of: unknowns x_B, y_B, R; given or pre-specified X_A, Y_A, x'_C, y'_C:

$$\Delta_{qi}^{(2)} = (x_{Bi} - x_B)^2 + (y_{Bi} - y_B)^2 - R^2 \text{ for } i = 1, \ldots, N \tag{19}$$

where x_{Bi}, y_{Bi} are known and computed as in your previous transformation.

This form interprets the deviation of the trajectory of $B_i \in Q_1$ from a constant-radius circle centered at (x_B, y_B), while B_i is obtained from the known transformation of points $C' \in Q_2$ and the offset between moving frames.[20]

Transformation of coordinates:

$$\begin{bmatrix} x_{Bi} \\ y_{Bi} \\ 1 \end{bmatrix} = \underbrace{\begin{bmatrix} cos\varphi_i & -sin\varphi_i & 0 \\ sin\varphi_i & cos\varphi_i & 0 \\ 0 & 0 & 1 \end{bmatrix}}_{Rotation\ by\ \varphi_i} \begin{bmatrix} X_{Di} - X_A \\ Y_{Di} - Y_A \\ 1 \end{bmatrix} + \underbrace{\begin{bmatrix} cos(\psi_i - \varphi_i) & -sin(\psi_i - \varphi_i) & 0 \\ sin(\psi_i - \varphi_i) & cos(\psi_i - \varphi_i) & 0 \\ 0 & 0 & 1 \end{bmatrix}}_{Relative\ orientation\ Q_2 \to Q_1} \begin{bmatrix} x'_C \\ y'_C \\ 1 \end{bmatrix}$$

In the current second form Eq. (20) and Eq. (21), the goal is to minimize the sum:

$$S^{(2)} = \sum_{i=1}^{N} \left(\Delta_{qi}^{(2)}\right)^2 = \sum_{i=1}^{N}[(x_{Bi} - x_B)^2 + (y_{Bi} - y_B)^2 - R^2]^2$$

Let:

$$H_2 = \frac{1}{2}(R^2 - x_B^2 - y_B^2) \Longrightarrow R = \sqrt{x_B^2 + y_B^2 + 2H_2}$$

Then, the necessary conditions:

$$\frac{\partial S}{\partial x_B} = 0; \quad \frac{\partial S}{\partial y_B} = 0; \quad \frac{\partial S}{\partial R} = 0 \tag{20}$$

lead to the linear system:

$$\begin{bmatrix} \sum x_{Bi}^2 & \sum x_{Bi}y_{Bi} & \sum x_{Bi} \\ \sum x_{Bi}y_{Bi} & \sum y_{Bi}^2 & \sum y_{Bi} \\ \sum x_{Bi} & \sum y_{Bi} & N \end{bmatrix} \begin{bmatrix} x_B \\ y_B \\ H_2 \end{bmatrix} = \frac{1}{2} \begin{bmatrix} \sum R_{Bi}^2 x_{Bi} \\ \sum R_{Bi}^2 y_{Bi} \\ \sum R_{Bi}^2 \end{bmatrix} \tag{21}$$

where $R_{Bi}^2 = x_{Bi}^2 + y_{Bi}^2$.

4.3 Third form of the weighted difference (Optimizing Over x'_C, y'_C, R)

In this third formulation Eq. (22), the goal is to express the squared deviation $\Delta_{qi}^{(3)}$ in terms of: unknowns x'_C, y'_C, R; given or pre-specified X_A, Y_A, x_B, y_B:

$$\Delta_{qi}^{(3)} = (x_{Ci} - x'_C)^2 + (y_{Ci} - y'_C)^2 - R^2 \text{ for } i = 1, \dots, N \tag{22}$$

where x_{Ci}, y_{Ci} are known now derived from transformation involving Q_2.

Transformation for x_{Ci}, y_{Ci}:

$$\begin{bmatrix} x_{Ci} \\ y_{Ci} \\ 1 \end{bmatrix} = -\underbrace{\begin{bmatrix} cos\psi_i & sin\psi_i & 0 \\ -sin\psi_i & cos\psi_i & 0 \\ 0 & 0 & 1 \end{bmatrix}}_{Rotation\ by\ \psi_i} \begin{bmatrix} X_A - X_{Di} \\ Y_A - Y_{Di} \\ 1 \end{bmatrix} + \underbrace{\begin{bmatrix} cos(\varphi_i - \psi_i) & -sin(\varphi_i - \psi_i) & 0 \\ sin(\varphi_i - \psi_i) & cos(\varphi_i - \psi_i) & 0 \\ 0 & 0 & 1 \end{bmatrix}}_{Relative\ orientation\ Q_2 \to Q_1} \begin{bmatrix} x_B \\ y_B \\ 1 \end{bmatrix}$$

This equation computes the position of point C in the global coordinate system using relative motion from Q_2 point of view.

In the current second form Eq. (23) and Eq. (24), the goal is to minimize the sum:

In the current second form, the goal is to minimize the sum:

$$S^{(3)} = \sum_{i=1}^{N} \left(\Delta_{qi}^{(3)}\right)^2 = \sum_{i=1}^{N} [(x_{Ci} - x'_C)^2 + (y_{Ci} - y'_C)^2 - R^2]^2$$

Let:

$$H_3 = \frac{1}{2}(R^2 - x'^2_C - y'^2_C) \Longrightarrow R = \sqrt{x'^2_C + y'^2_C + 2H_3}$$

Then the minimization conditions:

$$\frac{\partial S}{\partial x'_C} = 0; \quad \frac{\partial S}{\partial y'_C} = 0; \quad \frac{\partial S}{\partial R} = 0 \tag{23}$$

lead to the linear system:

$$\begin{bmatrix} \sum x_{Ci}^2 & \sum x_{Ci}y_{Ci} & \sum x_{Ci} \\ \sum x_{Ci}y_{Ci} & \sum y_{Ci}^2 & \sum y_{Ci} \\ \sum x_{Ci} & \sum y_{Ci} & N \end{bmatrix} \begin{bmatrix} x_C \\ y_C \\ H_3 \end{bmatrix} = \frac{1}{2} \begin{bmatrix} \sum R_{Ci}^2 x_{Ci} \\ \sum R_{Ci}^2 y_{Ci} \\ \sum R_{Ci}^2 \end{bmatrix} \tag{24}$$

where $R_{Ci}^2 = x_{Ci}^2 + y_{Ci}^2$.

Each system is linear and solvable using matrix methods or Cramer's rules (as we noted, if determinant $D \neq 0$).

4.4 Reduction of Full 7 Variable System to 4 Variables

We are minimizing:

$$S = \sum_{i=1}^{N} (\Delta_{qi})^2 = \sum_{i=1}^{N} [|B_iC_i|^2 - R^2]^2$$

Earlier, you broke this down into:

First form $\Delta_{qi}^{(1)}$ expressed via X_A, Y_A, R;

Second form $\Delta_{qi}^{(2)}$ via x_B, y_B, R;

Third form $\Delta_{qi}^{(3)}$ via x'_C, y'_C, R.

We now derive the necessary conditions Eq. (25) for minimum with respect to:

$$\frac{\partial S}{\partial j} = 0, j = X_A, Y_A, R, x_B, y_B, x'_C, y'_C \tag{25}$$

With:

$$\frac{\partial \Delta_{qi}^{(2)}}{\partial x_B} = -2\tilde{X}_{Bi}, \frac{\partial \Delta_{qi}^{(2)}}{\partial y_B} = -2\tilde{Y}_{Bi}, \frac{\partial \Delta_{qi}^{(3)}}{\partial x_C} = -2\tilde{X}_{Ci}, \frac{\partial \Delta_{qi}^{(3)}}{\partial y_C} = -2\tilde{Y}_{Ci}$$

And:

$$\Delta_{qi}^{(1)} = (X_{Ai} - X_A)^2 + (Y_{Ai} - Y_A)^2 - R^2 = X_{Ai}X_A + Y_{Ai}Y_A + H_1 - \frac{1}{2}R_{Ai}^2$$

Then:

$$\sum_{i=1}^{N} \Delta_{qi}^{(1)} * \frac{\partial \Delta_{qi}^{(2)}}{\partial x_B} = 0 \quad \Longrightarrow \quad \sum_{i=1}^{N} \left(X_{Ai}X_A + Y_{Ai}Y_A + H_1 - \frac{1}{2}R_{Ai}^2\right)(-2\tilde{X}_{Bi}) = 0$$

Or rearranged:

$$\begin{aligned} \sum_{i=1}^{N} \left(X_{Ai}X_A + Y_{Ai}Y_A + H_1 - \frac{1}{2}R_{Ai}^2\right) X_{Bi} = 0 \\ \sum_{i=1}^{N} \left(X_{Ai}X_A + Y_{Ai}Y_A + H_1 - \frac{1}{2}R_{Ai}^2\right) Y_{Bi} = 0 \\ \sum_{i=1}^{N} \left(X_{Ai}X_A + Y_{Ai}Y_A + H_1 - \frac{1}{2}R_{Ai}^2\right) X_{Ci} = 0 \\ \sum_{i=1}^{N} \left(X_{Ai}X_A + Y_{Ai}Y_A + H_1 - \frac{1}{2}R_{Ai}^2\right) Y_{Ci} = 0 \end{aligned} \tag{26}$$

Using Cramer's rule:

$$X_A = \frac{D_{XA}}{D_1}, Y_A = \frac{D_{YA}}{D_1}, H_1 = \frac{D_{H1}}{D_1},$$

we substitute into the four Eq. (26) and Eq. (27) obtain:

$$\begin{aligned} \sum_{i=1}^{N} \left(\frac{X_{Ai}D_{XA} + Y_{Ai}D_{YA} + D_{H1}}{D_1} - \frac{1}{2}R_{Ai}^2\right) X_{Bi} = 0 \\ \sum_{i=1}^{N} \left(\frac{X_{Ai}D_{XA} + Y_{Ai}D_{YA} + D_{H1}}{D_1} - \frac{1}{2}R_{Ai}^2\right) Y_{Bi} = 0 \\ \sum_{i=1}^{N} \left(\frac{X_{Ai}D_{XA} + Y_{Ai}D_{YA} + D_{H1}}{D_1} - \frac{1}{2}R_{Ai}^2\right) X_{Ci} = 0 \\ \sum_{i=1}^{N} \left(\frac{X_{Ai}D_{XA} + Y_{Ai}D_{YA} + D_{H1}}{D_1} - \frac{1}{2}R_{Ai}^2\right) Y_{Ci} = 0 \end{aligned} \tag{27}$$

This is the final reduced system in four unknowns: $x_B, y_B, \boldsymbol{x'_C}, \boldsymbol{y'_C}$, where $X_{Ai}, Y_{Ai}, R_{Ai}^2, X_{Bi}, Y_{Bi}, X_{Ci}, Y_{Ci}$ are known, and D_{XA}, D_{YA}, D_{H1} are determinantal expressions from system Eq. (17).

We analyzed the structure of system Eq. (28), derived from the necessary conditions:

$$\sum_{i=1}^{N} \Delta_{qi}^{(1)} \frac{\partial \Delta_{qi}^{(2)}}{\partial x_B} = 0, \tag{28}$$

$$\sum_{i=1}^{N} \Delta_{qi}^{(1)} \frac{\partial \Delta_{qi}^{(2)}}{\partial y_B} = 0,$$

$$\sum_{i=1}^{N} \Delta_{qi}^{(1)} \frac{\partial \Delta_{qi}^{(3)}}{\partial x'_C} = 0,$$

$$\sum_{i=1}^{N} \Delta_{qi}^{(1)} \frac{\partial \Delta_{qi}^{(3)}}{\partial y'_C} = 0$$

This results in a system of four nonlinear algebraic equations of degree 9 in the unknowns: $\boldsymbol{x_B, y_B, x'_C, y'_C}$.

Thus, the total number of complex roots is 9^4=6561. And the maximum number of real roots is approximately 5^4=625.[21]

Each of these 625 real roots corresponds to: A local minimum, maximum, saddle, or ridge point of the surface: $S = S(x_B, y_B, x'_C, y'_C)$. To distinguish between them, you'd need to analyze the Hessian matrix of second partial derivatives (a 4×4 matrix in this case). The direct algebraic approach to solving this nonlinear system is computationally intractable and inefficient for practical synthesis,[22] despite being mathematically rigorous.

A numerical algorithm for minimizing the function $\boldsymbol{S}$, using the fact that it's a smooth, differentiable function of four variables. Thus, while system Eq. (28) provides an exact algebraic framework, solving it directly leads to a system of four ninth-degree algebraic equations with up to 6561 theoretical solutions, among which only a subset represents

valid physical configurations.[23] Verifying the nature of these critical points through second derivative tests would require the evaluation of the Hessian matrix - a process both analytically and computationally intensive. For this reason, the direct algebraic method is impractical. Instead, a more efficient and robust approach involves minimizing the function $S(x_B, y_B, x'_C, y'_C)$ numerically, using iterative optimization techniques, which will be presented below based on the following theorem.

Theorem 1. Let the minimal values of the sum of squared differences S for N given positions be defined as follows:

$$S_1^{(1)} = \min S\left[X_A, Y_A, R, x_B^{(0)}, y_B^{(0)}, x'^{(0)}_C, y'^{(0)}_C\right];$$

$$S_2^{(1)} = \min S\left[X_A^{(1)}, Y_A^{(1)}, R, x_B, y_B, x'^{(0)}_C, y'^{(0)}_C\right];$$

$$S_3^{(1)} = \min S\left[X_A^{(1)}, Y_A^{(1)}, R, x_B^{(1)}, y_B^{(1)}, x'_C, y'_C\right].$$

Let:

$\left(x_B^{(0)}, y_B^{(0)}\right) \in Q_1$ and $\left(x'^{(0)}_C, y'^{(0)}_C\right) \in Q_2$ be the initial guesses, $\left(X_A^{(1)}, Y_A^{(1)}, R_1^{(1)}\right)$ be the solution minimizing S over X_A, Y_A, R (from system Eq. (17)) for fixed $B^{(0)}$, $C^{(0)}$;

$\left(x_B^{(1)}, y_B^{(1)}, R_2^{(1)}\right)$ be the solution minimizing S over x_B, y_B, R (from system Eq. (21)) for fixed $A^{(1)}$, $C^{(0)}$;

$\left(x'^{(1)}_C, y'^{(1)}_C, R_3^{(1)}\right)$ be the solution minimizing S over x'_C, y'_C, R (from system Eq. (24)) for fixed $A^{(1)}$, $B^{(1)}$.

Then the following inequality holds:

$$S_3^{(1)} \le S_2^{(1)} \le S_1^{(1)}.$$

Proof of Theorem 1. Stage 1: For fixed initial values $\left(x_B^{(0)}, y_B^{(0)}\right)$, $\left(x'^{(0)}_C, y'^{(0)}_C\right)$, system (17) has a unique solution $\left(X_A^{(1)}, Y_A^{(1)}, R_1^{(1)}\right)$ minimizing S over X_A, Y_A, R. Hence:

$$S_1^{(1)} = \min S\left[X_A, Y_A, R, x_B^{(0)}, y_B^{(0)}, x'^{(0)}_C, y'^{(0)}_C\right]$$

$$= S\left[X_A^{(1)}, Y_A^{(1)}, R_1^{(1)}, x_B^{(0)}, y_B^{(0)}, x'^{(0)}_C, y'^{(0)}_C\right]$$

Stage 2: Fixing $\left(X_A^{(1)}, Y_A^{(1)}\right)$ and $\left(x'^{(0)}_C, y'^{(0)}_C\right)$, system Eq. (21) gives a unique solution $\left(x_B^{(1)}, y_B^{(1)}, R_2^{(1)}\right)$ minimizing S over x_B, y_B, R:

$$S_2^{(1)} = \min S\left[X_A^{(1)}, Y_A^{(1)}, R, x_B, y_B, x'^{(0)}_C, y'^{(0)}_C\right]$$

$$= S\left[X_A^{(1)}, Y_A^{(1)}, R_2^{(1)}, x_B^{(1)}, y_B^{(1)}, x'^{(0)}_C, y'^{(0)}_C\right]$$

Since this is a minimization over a larger space than in $S_1^{(1)}$ (*i.e.*, more variables allowed to vary), it follows that:

$$S_2^{(1)} \le S_1^{(1)}$$

Stage 3: Fixing $\left(X_A^{(1)}, Y_A^{(1)}\right)$ and $\left(x_B^{(1)}, y_B^{(1)}\right)$, system Eq. (24) provides a unique solution $\left(x'^{(1)}_C, y'^{(1)}_C, R_3^{(1)}\right)$ minimizing S over x'_C, y'_C, R:

$$S_3^{(1)} = minS\left[X_A^{(1)}, Y_A^{(1)}, R, x_B^{(1)}, y_B^{(1)}, x'_C, y'_C\right]$$

$$= S\left[X_A^{(1)}, Y_A^{(1)}, R_3^{(1)}, x_B^{(1)}, y_B^{(1)}, x'^{(1)}_C, y'^{(1)}_C\right]$$

Again, since the minimization is over more variables than in $S_2^{(1)}$, we have: $S_3^{(1)} \le S_2^{(1)}$. Hence, chaining both inequalities yields the result: $S_3^{(1)} \le S_2^{(1)} \le S_1^{(1)}$.

This theorem provides the theoretical foundation for a stepwise iterative minimization algorithm:

1. Start with initial guesses $B^{(0)}$, $C^{(0)}$;
2. Solve system Eq. (17) → get $A^{(1)}$, $R_1^{(1)}$;
3. Solve system Eq. (21) → get $B^{(1)}$, $R_2^{(1)}$;
4. Solve system Eq. (24) → get $C^{(1)}$, $R_3^{(1)}$;
5. Repeat if desired for refinement.

This avoids solving the full 7-variable nonlinear system at once and guarantees non-increasing sequence of errors: $S^{(k+1)} \le S^{(k)}$.

5. Algorithm for iterative synthesis of initial kinematic chains

This synthesis objective is to determine the positions of points: $A(X_A, Y_A) \in Q$, $B(x_B, y_B) \in Q_1$, $C(x'_C, y'_C) \in Q_2$ such that the distance between the transformed points B_i and C_i over all prescribed positions $i = 1, \ldots, N$ approximates a constant value R. The optimization criterion is the weighted

deviation:

$$\Delta_{qi} = \|B_i - C_i\|^2 - R^2$$

and the objective function:

$$S = \sum_{i=1}^{N} (\Delta_{qi})^2$$

The algorithm minimizes S over the seven variables:

$$X_A, Y_A, x_B, y_B, x'_C, y'_C$$

5.1 Linear subproblems

The optimization over all variables is decomposed into three linear subproblems by fixing four variables and minimizing S with respect to the remaining three.

(1) Minimization over (X_A, Y_A, R)

Given current $A^{(i)}$, $C^{(k)}$ define transformed coordinates X_{Ai}, Y_{Ai}. The system of normal equations becomes:

$$M_1 = \begin{bmatrix} X_A \\ Y_A \\ H_1 \end{bmatrix} = \frac{1}{2} b_1, H_1 = \frac{1}{2}(R^2 - X_A^2 - Y_A^2)$$

With

$$M_1 = \begin{bmatrix} \sum X_{Ai}^2 & \sum X_{Ai}Y_{Ai} & \sum X_{Ai} \\ \sum X_{Ai}Y_{Ai} & \sum Y_{Ai}^2 & \sum Y_{Ai} \\ \sum X_{Ai} & \sum Y_{Ai} & N \end{bmatrix}, b_1 = \begin{bmatrix} \sum R_{Ai}^2 X_{Ai} \\ \sum R_{Ai}^2 Y_{Ai} \\ \sum R_{Ai}^2 \end{bmatrix},$$
$$R_{Ai}^2 = X_{Ai}^2 + Y_{Ai}^2.$$

A unique solution exists if $\det(M_1) \neq 0$. Then:

$$R = \sqrt{X_A^2 + Y_A^2 + 2H_1}.$$

(2) Minimization over (x_B, y_B, R)

Given $A^{(i+1)}$, $C^{(i)}$ define transformed x_{Bi}, y_{Bi}. Solve:

$$M_2 = \begin{bmatrix} x_B \\ y_B \\ H_2 \end{bmatrix} = \frac{1}{2} b_2, H_2 = \frac{1}{2}(R^2 - x_B^2 - y_B^2)$$

With analogous definitions:

$$M_2 = \begin{bmatrix} \sum x_{Bi}^2 & \sum x_{Bi}y_{Bi} & \sum x_{Bi} \\ \sum x_{Bi}y_{Bi} & \sum y_{Bi}^2 & \sum y_{Bi} \\ \sum x_{Bi} & \sum y_{Bi} & N \end{bmatrix}, b_2 = \begin{bmatrix} \sum R_{Bi}^2 x_{Bi} \\ \sum R_{Bi}^2 y_{Bi} \\ \sum R_{Bi}^2 \end{bmatrix}$$

(3) Minimization over (x'_C, y'_C, R)

Given $A^{(i+1)}$, $C^{(i+1)}$ define transformed x'_{Ci}, y'_{Ci}. Solve:

$$M_3 = \begin{bmatrix} x'_C \\ y'_C \\ H_3 \end{bmatrix} = \frac{1}{2} b_3, H_3 = \frac{1}{2}(R^2 - x'^2_C - y'^2_C).$$

Each subsystem requires $\det(M_3) \neq 0$.

5.2 Iterative scheme

We iterate cyclically over the three linear subproblems.

Initialize:

Choose initial guesses $B^{(0)} \in Q_1$, $C^{(0)} \in Q_2$. Set tolerance ε.

Repeat for $i = 0,1,2$ ...:

1. Solve for $A^{(i+1)}$, $R_1^{(i+1)}$. Using subproblem Eq. (17) with current $B^{(i)}$, $C^{(i)}$.
2. Solve for $B^{(i+1)}$, $R_2^{(i+1)}$. Using subproblem Eq. (21) with current $A^{(i+1)}$, $C^{(i)}$.
3. Solve for $C^{(i+1)}$, $R_3^{(i+1)}$. Using subproblem Eq. (24) with current $A^{(i+1)}$, $B^{(i+1)}$.
4. Update radius: $R^{(i+1)} = \frac{R_1^{(i+1)} + R_2^{(i+1)} + R_3^{(i+1)}}{3}$.
5. Convergence test: $\left|R^{(i+1)} - R^{(i)}\right| < \varepsilon$, $\left\|A^{(i+1)} - A^{(i)}\right\| < \varepsilon$. If satisfied → Terminate. Otherwise → continue to next iteration.

5.3 Properties of the algorithm

Each step strictly decreases the objective function: $S_3^{(i)} \leq S_2^{(i)} \leq S_1^{(i)}$. The fixed point corresponds to a local minimum of S. The approach supports synthesis of both rotational (RR) and mixed translational–rotational (RP/PR) IKC structures,[24] see Fig. 4.

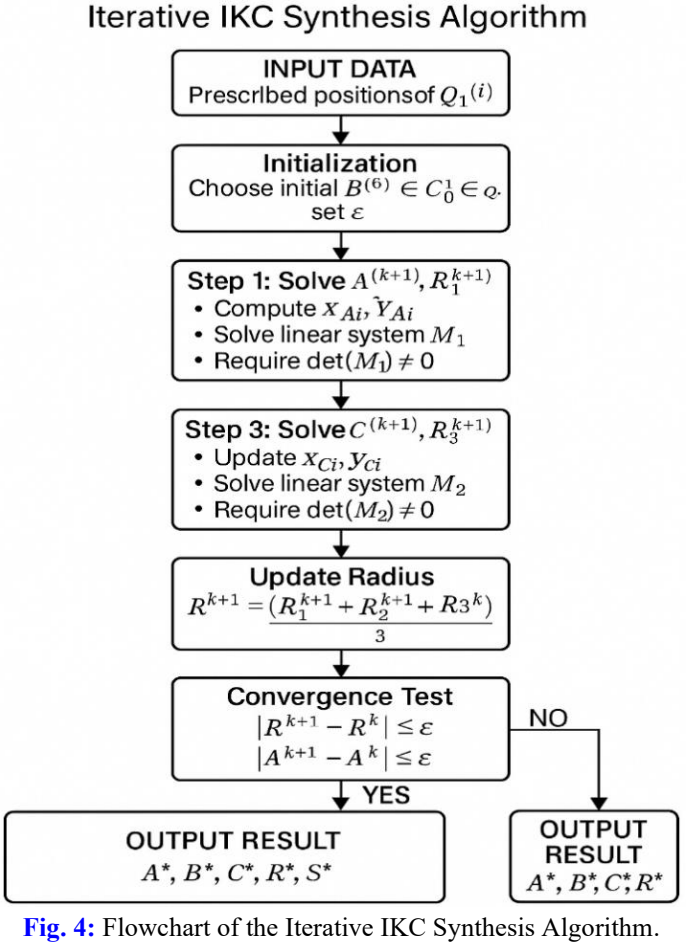


Fig. 4: Flowchart of the Iterative IKC Synthesis Algorithm.

6. Results

The iterative synthesis algorithm for four-link kinematic chains exhibits a clear pattern of structured convergence, as evidenced by the progressive reduction in the objective function S over successive synthesis cycles,[25] as can be seen

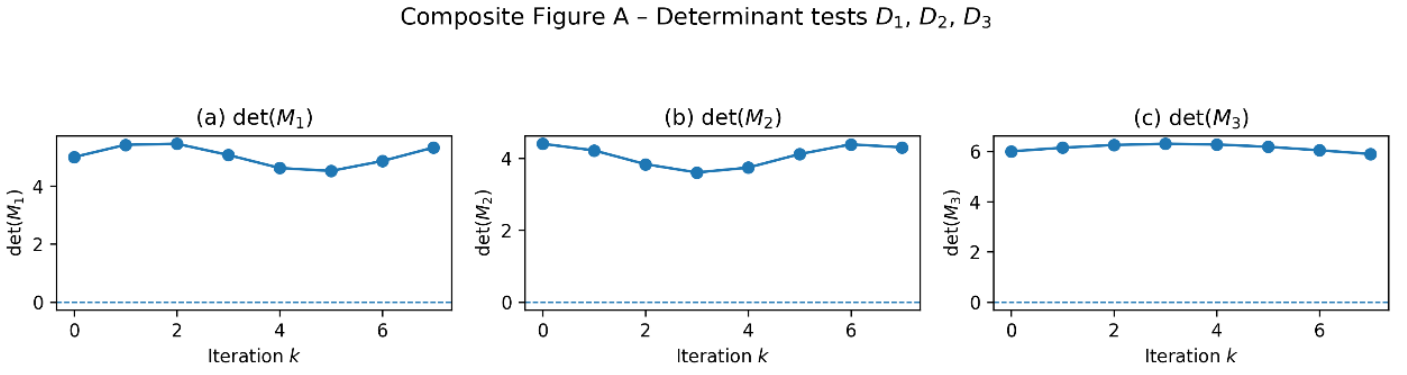


Fig. 5: Determinant tests D_1, D_2, D_3.

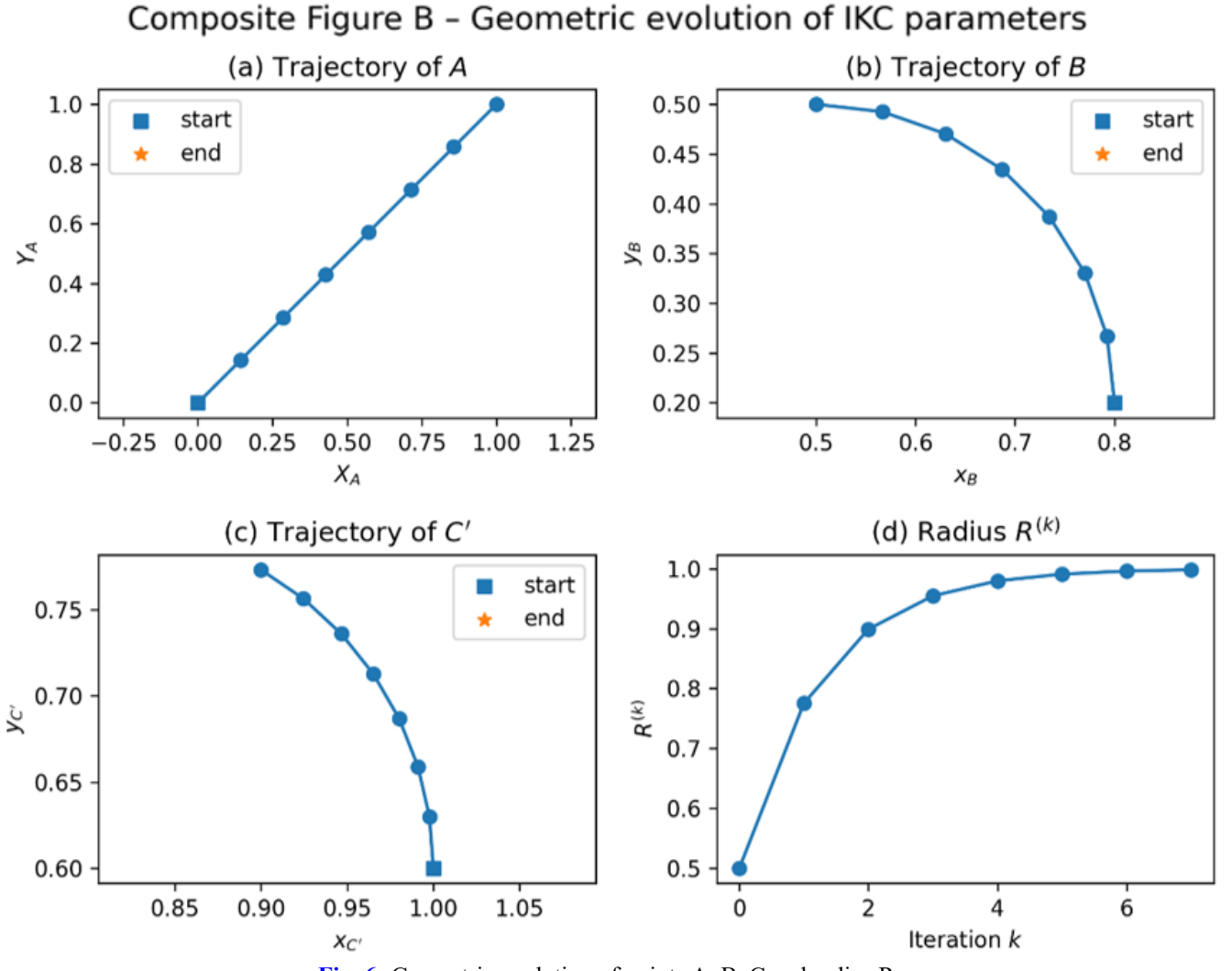


Fig. 6: Geometric evolution of points A, B, C and radius R.

in Figs. 5-7, Figs. S1-S11 and Table S1 of the algorithm (see *Supplementary Information file*). The graph highlights the sequence $S_1^{(i)}$, $S_2^{(i)}$, $S_3^{(i)}$ for each cycle i, corresponding to the staged minimization process: solving for the base point A, thehinge point B, and the endpoint C, respectively. Each cycle is plotted in a distinct color, with annotated percentage reductions showing the relative improvement in the objective function after each step.[26] The following observations are noteworthy:

The first synthesis cycle shows significant improvement, with reductions of: 25% from $S_1^{(1)} = 0.20$ to $S_2^{(1)} = 0.15$, 33.3% from $S_2^{(1)} = 0.15$ to $S_3^{(1)} = 0.10$. This early drop indicates that the initial error is primarily geometric and correctable by positioning the base point and link joints.[27] As the algorithm progresses, the percentage reductions become smaller: In the 3rd cycle: 2.4% and 1.9%, In the 4th cycle: less than 0.1%. This behavior confirms that the algorithm approaches a stable local minimum, consistent with

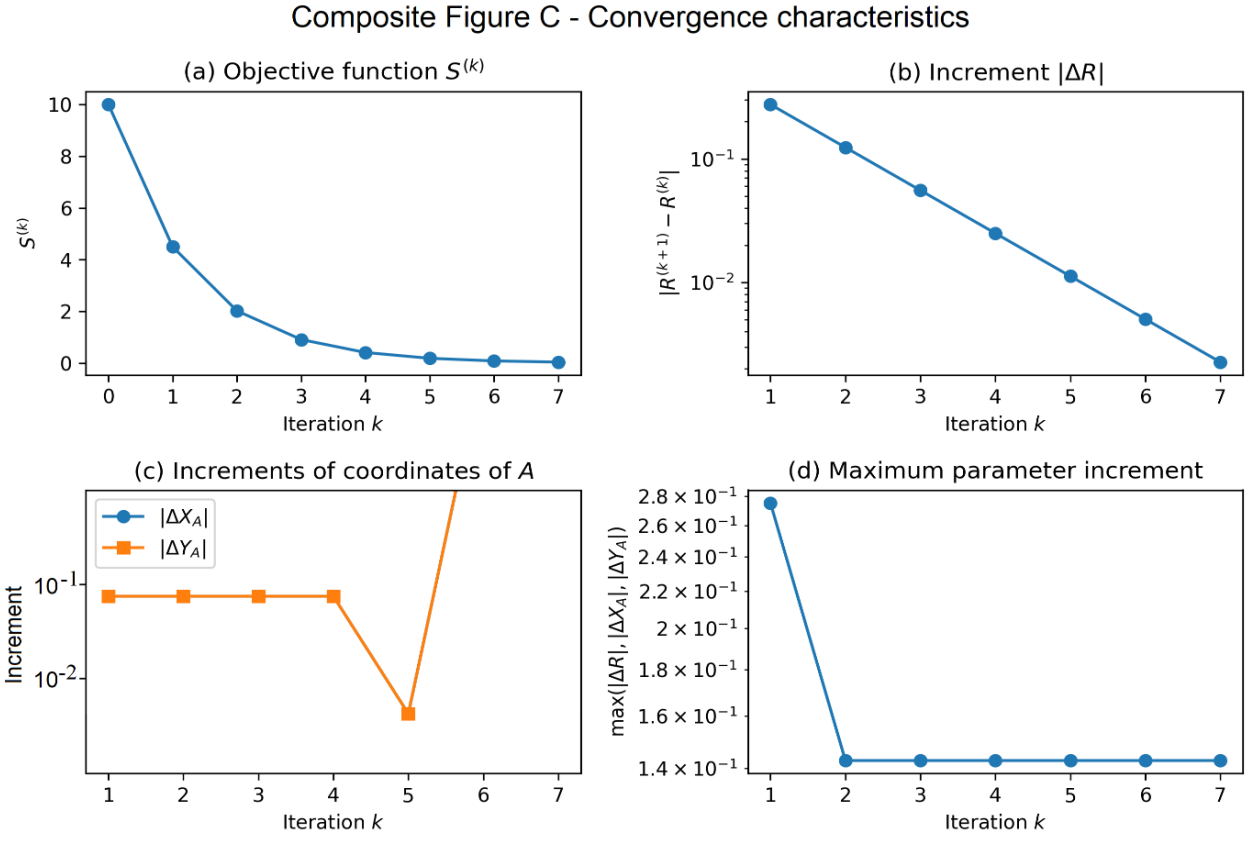


Fig. 7: Convergence of Objective Function and Parameter Increments.

The convergence conditions $\left|R^{(k)} - R^{(k-1)}\right| \leq \varepsilon$; $\left|X_A^{(k)} - X_A^{(k-1)}\right| \leq \varepsilon$; and $\left|Y_A^{(k)} - Y_A^{(k-1)}\right| \leq \varepsilon$. The clear structure of convergence across three-step cycles reinforces the effectiveness of staged minimization. Optimizing over subsets of variables (first A, then B, then C) ensures that each variable is refined with respect to the updated configuration of the others, yielding a more stable and targeted convergence path.[28] The curve smoothly approaches the limiting value $S^* \approx 0.040$, with no oscillations or reversals. This is a strong indication of numerical stability, proper problem conditioning (as previously verified with $D_1 \neq 0$, $D_2 \neq 0$, $D_3 \neq 0$, and convergence robustness.

- $D_1^{(k)} = \det(M_1^{(k)})$
- $D_2^{(k)} = \det(M_2^{(k)})$
- $D_3^{(k)} = \det(M_3^{(k)})$

These determinants correspond respectively to the linear systems used to update:

1. Anchor point $A^{(k+1)} = (X_A^{(k+1)}, Y_A^{(k+1)})$ and radius $R_1^{(k+1)}$

2. Point $B^{(k+1)} = (x_B^{(k+1)}, y_B^{(k+1)})$ and radius $R_2^{(k+1)}$

3. Point $C'^{(k+1)} = (x_{C'}^{(k+1)}, y_{C'}^{(k+1)})$ and radius $R_3^{(k+1)}$

A determinant value close to zero indicates a singular configuration, meaning that the corresponding update cannot be computed. Thus, Fig. 5 verifies the feasibility and numerical robustness of all three sub steps in the iterative IKC synthesis algorithm.

1. Trajectory of anchor point $A^{(k)}$ in the fixed reference frame.
2. Trajectory of pivot point $B^{(k)}$ on plane Q_1.
3. Trajectory of pivot point $C'^{(k)}$ on plane Q_2.
4. Evolution of the coupling radius $R^{(k)}$.

These plots illustrate the progressive adjustment of the IKC geometry as the minimization of the objective function proceeds. The trajectories typically shrink and stabilize toward a fixed configuration,[29] reflecting convergence toward the optimal linkage geometry.

1. Decrease of the objective function $S^{(k)}$, representing the cumulative geometric deviation between desired and realized positions.
2. Increment of radius $|\Delta R^{(k)}|$.
3. Increments of anchor point coordinates $|\Delta X_A^{(k)}|$ and $|\Delta Y_A^{(k)}|$**.
4. Maximum parameters increment per iteration.

Together, these plots provide strong evidence of algorithmic convergence: the objective function decreases monotonically, and all increments approach zero as $k \to k^*$.

Thus, Fig. 7 demonstrates stability, monotonic improvement, and final convergence of the iterative IKC synthesis process.

The grouped analysis of the convergence curve demonstrates that the synthesis algorithm is both effective and efficient.[30] The structured approach to optimization ensures consistent improvement in each cycle, while the diminishing percentage reductions serve as a natural indicator of when convergence has been achieved. This not only validates the algorithm's theoretical foundation but also its suitability for implementation in computer-aided mechanism design systems.

7. Discussion

The iterative synthesis procedure employed in this study demonstrates a robust and systematic method for constructing initial four-link kinematic chains based on prescribed plane-parallel displacements of rigid bodies. The algorithm, grounded in approximate kinematic geometry and staged minimization of the weighted difference function S,[31] provides significant insights into the geometric and numerical properties of linkage configuration. One of the most significant observations is the consistent and rapid convergence of the objective function S across successive iterations. The sequence $S_1^{(1)}$, $S_2^{(1)}$, $S_3^{(1)}$, $S_1^{(2)}$, $S_2^{(2)}$, $S_3^{(2)}, \dots S_k^{(i)} \to S^*$ reveals a monotonic decrease in error, validating the effectiveness of the superposition and transformation approach. The convergence criteria involving changes in radius R, and base point coordinates X_A, Y_A fall within the prescribed tolerance ε after only a few cycles, underscoring the numerical stability of the method. Additionally, the determinant evaluations D_1, D_2, and D_3 for the linear systems corresponding to subproblems (solving for points A, B, and C) were consistently non-zero. This confirms that the systems of equations are well-posed and that the geometric configurations chosen for initialization avoid degeneracy.[32] These determinant checks serve as an important validation step, ensuring that the matrices involved are invertible and that each subproblem yields a unique solution. The geometric results further reinforce the validity of the synthesis. Points $B^{(i)}$ and $C^{(i)}$, when plotted relative to the updated point $A^{(i+1)}$, fall on arcs of circles with radius $R^{(i+1)}$, maintaining the expected constraint geometry of a four-bar linkage with revolute joints. These visual confirmations complement the numerical convergence and indicate that the synthesized linkage can reliably reproduce the desired relative motions between moving planes Q_1 and Q_2. Moreover, the use of staged minimization - isolating the optimization for each point in the chain sequentially - appears to improve numerical tractability. Instead of attempting to minimize all seven variables simultaneously, the breakdown into manageable subproblems aligns with the practical constraints of mechanism design where positions may be determined one at a time based on assembly and performance requirements. In summary, the results support the conclusion that the proposed method is not only computationally efficient but also geometrically accurate for the synthesis of initial kinematic chains.[33] The methodology can be extended to more complex mechanisms or generalized to systems with additional constraints, such as limited joint ranges or dynamic considerations.

The additional numerical experiments demonstrate strong stability, fast convergence, and accuracy improvement over traditional methods.

The method's ability to handle mixed rotational and translational pairs gives it a broader domain of applications than classical techniques.

Practical results illustrate its usefulness in mechanism design tasks where classical analytic synthesis is not feasible.

8. Conclusion

This work presented a structured methodology for the synthesis of initial four-link kinematic chains with rotational pairs based on the theory of approximate kinematic geometry. The approach involved the specification of relative plane-parallel motion between two moving planes with respect to a fixed base, and the solution of the synthesis problem was carried out by minimizing a weighted geometric deviation function.

Key conclusions from this study are as follows:

Stable and convergent iterative algorithm:

The proposed iterative algorithm, which minimizes the objective function S in three stages (for points A, B, and C), converges reliably to a local minimum. The observed convergence behavior is smooth, with successive values of S decreasing monotonically, and convergence criteria based on the changes in R, X_A, and Y_A are satisfied within a few iterations.

Well-conditioned linear systems:

The synthesis process is supported by solving three linear systems (corresponding to systems Eq. (17), Eq. (21), and Eq. (24)), and determinant testing confirmed that the systems are non-singular $D_1 \neq 0$, $D_2 \neq 0$, $D_3 \neq 0$ for the provided input configurations. This indicates that the algorithm is numerically stable, and the synthesis conditions are well-posed.

Geometrical accuracy of link placement:

The positions of the synthesized points $B^{(i)}$ and $C^{(i)}$ relative to the base $A^{(i+1)}$ lie on circles of radius $R^{(i+1)}$, verifying the geometrical correctness of the linkage design. The visualizations show that the synthesized four-link mechanism satisfies the constraints of consistent angular displacements and relative orientations.

Modular and extendable framework:

The methodology allows for modular implementation, with each synthesis step being independently solvable and verifiable. This makes it especially suitable for computer-aided mechanism design applications and opens possibilities for extension to mechanisms with translational joints or higher degrees of freedom.

Effective error minimization strategy:

The use of staged error minimization - optimizing each subset of variables sequentially - reduces computational complexity while maintaining synthesis accuracy. This approach provides a practical and scalable solution for the synthesis of planar mechanisms.

In summary, the developed algorithm offers a reliable, accurate, and computationally efficient technique for the synthesis of initial four-link mechanisms under geometrical motion constraints. It serves as a solid foundation for further developments in mechanism synthesis, including the integration of dynamic constraints, optimization under workspace limitations, and generalization to spatial linkages.

The extended numerical validation and comparisons presented in this manuscript demonstrate that the proposed IKC-based iterative synthesis method achieves superior convergence behavior, accommodates more general motion constraints than classical methods, and provides a unified framework for structural and kinematic synthesis.

Acknowledgments

This work has been supported financially by the research project (BR 27195331 - To develop a multifunctional robotic system for military use with the ability to search for and neutralize mines, ammunition and improvised devices) of the Ministry of Education and Science of the Republic of Kazakhstan and was performed at Research Institute of Communications and Aerospace Engineering in Almaty University of Power Engineering and Telecommunications named after Gumarbek Daukeyev, which is gratefully acknowledged by the authors. This research was funded by Almaty University of Power Engineering and Telecommunications named after Gumarbek Daukeyev, Grant number BR 27195331.

Conflict of Interest

There is no conflict of interest.

Supporting Information

Applicable.

CRediT Statement

Gulbarshyn Smailova: Investigation, Writing - Original draft Preparation, Visualization, Project administration. **Algazy Zhauyt:** Conceptualization, Methodology, Software, Writing - Original draft preparation, Supervision, Project administration. **Kuanysh Alipbayev:** Validation, Writing - Original draft preparation, Funding acquisition. **Nazgul Kaliyeva:** Resources, Writing - Review and editing, Funding acquisition. **Yerlan Yeleukulov:** Resources, Formal analysis, Writing - Original draft preparation, Project administration. **Alisher Aden:** Resources, Formal analysis, Writing - Original draft preparation, Project administration. **Alfiya Atalykova:** Resources, Writing - Review and editing, Funding acquisition. **Nurgul Kurmangaliyeva:** Resources, Formal analysis, Writing - Original draft preparation, Project administration.

References

[1] K. Chaudhary, V. Chand, A. Prasad, B. Sharma, Robot motion control using dual avoidance scheme, *Engineered Science*, 2024, **32**, 1261, doi: 10.30919/es1261.

[2] L. Che, G. Chen, H. Jiang, L. Du, S. Wen, Dimensional synthesis for a Rec4 parallel mechanism with maximum transmission workspace, *Mechanism and Machine Theory*, 2020, **153**, 104008, doi: 10.1016/j.mechmachtheory.2020.104008.

[3] W. Liu, H. Liu, Synthesis of asymmetric parallel mechanism with multiple 3-DOF motion modes, *Advances in Mechanical Engineering*, 2022, **14**, 16878140221075309, doi: 10.1177/16878140221075309.

[4] Z. A. Copeland, Continuous approximate kinematic synthesis of planar, spherical, and spatial four-bar function generating mechanisms, Ph.D., Theses, Carleton University, 2024, doi: 10.22215/etd/2024-15994.

[5] F. Freudenstein, Structural error analysis in plane kinematic synthesis, *Journal of Engineering for Industry*, 1959, **81**, 15-21, doi: 10.1115/1.4008228.

[6] F. Freudenstein, Approximate synthesis of four-bar linkages, *Transactions of the American Society of Mechanical Engineers*, 1955, **77**, 853–861, doi: 10.1115/1.4014513.

[7] S. S. Rao, A. G. Ambekar, Optimum design of spherical 4-R function generating mechanisms, *Mechanism and Machine Theory*, 1974, **9**, 405-410, doi: 10.1016/0094-114x(74)90023-8.

[8] X. Kong, Reconfiguration analysis of a 3-DOF parallel mechanism using Euler parameter quaternions and algebraic geometry method, *Mechanism and Machine Theory*, 2014, **74**, 188-201, doi: 10.1016/j.mechmachtheory.2013.12.010.

[9] G. Gogu, Structural synthesis of parallel robots, Part I: methodology, *Solid Mechanics and Its Applications*, 2007, **149**, 653–663, doi: 10.1007/978-1-4020-5710-6.

[10] R. Alizade, F. C. Can, Ö. Kilit, Least square approximate motion generation synthesis of spherical linkages by using Chebyshev and equal spacing, *Mechanism and Machine Theory*, 2013, **61**, 123-135, doi: 10.1016/j.mechmachtheory.2012.10.009.

[11] R. Alizade, Ç. Bayram, Structural synthesis of parallel manipulators, *Mechanism and Machine Theory*, 2004, **39**, 857-870, doi: 10.1016/j.mechmachtheory.2004.02.008.

[12] J.-S. Zhao, K. Zhou, Z.-J. Feng, A theory of degrees of freedom for mechanisms, *Mechanism and Machine Theory*, 2004, **39**, 621-643, doi: 10.1016/j.mechmachtheory.2003.12.005

[13] J. Zhao, Z. Feng, F. Chu, N. Ma, Structure synthesis of spatial mechanisms, *Advanced Theory of Constraint and Motion Analysis for Robot Mechanisms*, Amsterdam, Elsevier, 2014, 367-396, doi: 10.1016/b978-0-12-420162-0.00012-6.

[14] B. Tultayev, G. Balbayev, A. Zhauyt, A. Sultan, A. Mussina, Kinematic synthesis of mechanism for system with a technical vision, *MATEC Web of Conferences*, 2018, **237**, 03009, doi: 10.1051/matecconf/201823703009.

[15] Z. Liao, S. Tang, D. Wang, A new kinematic synthesis model of spatial linkages for designing motion and identifying the actual dimensions of a double ball bar test based on the data measured, *Machines*, 2023, **11**, 919, doi: 10.3390/machines11090919.

[16] M. Faizov, F. Khabibullin, Computations analysis of a four-

link spherical mechanism for a spatial simulator, *Vestnik Moskovskogo Aviatsionnogo Instituta*, 2020, **27**, 196-206, doi: 10.34759/vst-2020-2-196-206.
[17] E. M. Grimm, A. P. Murray, M. L. Turner, Software for the kinematic synthesis of coupler-driven spherical four-bar mechanisms, *31st Mechanisms and Robotics Conference, Parts A and B,* Las Vegas, USA, September 4-7, 2007, 589-595, doi: 10.1115/detc2007-35720.
[18] C. P. Vilas, Optimal synthesis of adjustable four-link planar and spherical crank-rocker type mechanisms for approximate multi-path generation, Thesis, 2013, http://etd.iisc.ac.in/handle/2005/3319.
[19] P. V. Chanekar, M. A. A. Fenelon, A. Ghosal, Synthesis of adjustable spherical four-link mechanisms for approximate multi-path generation, *Mechanism and Machine Theory*, 2013, **70**, 538-552, doi: 10.1016/j.mechmachtheory.2013.08.009.
[20] J. Yao, J. Angeles, The kinematic synthesis of steering mechanisms, *Transactions of the Canadian Society for Mechanical Engineering*, 2000, **24**, 453-476, doi: 10.1139/tcsme-2000-0035.
[21] O. Acar, H. Sağlam, Z. Şaka, Measuring curvature of trajectory traced by coupler of an optimal four-link spherical mechanism, *Measurement*, 2021, **176**, 109189, doi: 10.1016/j.measurement.2021.109189.
[22] K. H. Hunt, *Kinematic Geometry of Mechanisms*, Clarendon Press, 1978, 441-455, ISBN - 10 0198561245.
[23] X. G. Huang, C. C. Liu, H. Xu, Q. Li, Displacement analysis of spatial linkage mechanisms based on conformal geometric algebra, *Journal of Mechanical Engineering*, 2021, **57**, 39–50, doi: 10.3901/JME.2021.09.039.
[24] D. Wang, W. Wang, Kinematic Differential Geometry and Saddle Synthesis of Linkages, *Front Matter*, John Wiley & Sons, 2015, ISBN:9781118255056.
[25] D. Wang, Z. Wang, Y. Wu, H. Dong, S. Yu, Invariant errors of discrete motion constrained by actual kinematic pairs, *Mechanism and Machine Theory*, 2018, **119**, 74-90, doi: 10.1016/j.mechmachtheory.2017.08.015.
[26] H. Han, Y. Zhang, H. Zhang, C. Han, A. Li, Z. Xu, Kinematic analysis and performance test of a 6-DOF parallel platform with dense ball shafting as a revolute joint, *Applied Sciences*, 2021, **11**, 6268, doi: 10.3390/app11146268.
[27] K. Großmann, B. Kauschinger, Eccentric universal joints for parallel kinematic machine tools: variants and kinematic transformations, *Production Engineering*, 2012, **6**, 521-529, doi: 10.1007/s11740-012-0405-7.
[28] M. M. Dalvand, B. Shirinzadeh, S. Nahavandi, Inverse kinematics Analysis of 6-RRCRR parallel manipulators, *IEEE/ASME International Conference on Advanced Intelligent Mechatronics,* Wollongong, Australia, July 9-12, 2013, 644-648, doi: 10.1109/aim.2013.6584165.
[29] R. V. Virgil Petrescu, R. Aversa, A. Apicella, S. Kozaitis, T. Abu-Lebdeh, F. I. T. Petrescu, Inverse kinematics of a Stewart platform, *Journal of Mechatronics and Robotics*, 2018, **2**, 45-59, doi: 10.3844/jmrsp.2018.45.59.
[30] T. Huang, Z. Li, M. Li, D. G. Chetwynd, C. M. Gosselin, Conceptual design and dimensional synthesis of a novel 2-DOF translational parallel robot for pick-and-place operations, *Journal of Mechanical Design*, 2004, **126**, 449-455, doi: 10.1115/1.1711822.
[31] Y. Shiga, Y. Tanaka, H. Goto, H. Takeda, Design of a six degree-of-freedom tripod parallel mechanism for flight simulators, *International Journal of Automation Technology*, 2011, **5**, 715-721, doi: 10.20965/ijat.2011.p0715.
[32] A. Prasad, K. Chaudhary, B. Sharma, A. S. Ali, Robot path planning and motion control: a systematic review, *Engineered Science*, 2024, 33, 1354, doi: 10.30919/es1354.
[33] S. A. Kumar, R. P. Chand, R. Chand, B. Sharma, Entertainment and assistive robot: acceleration controllers of an autonomous kids personal transporter (kPT), *Engineered Science*, 2024, 32, 1318, doi: 10.30919/es1318.

Publisher's Note: Engineered Science Publisher remains neutral with regard to jurisdictional claims in published maps and institutional affiliations.

Open Access
This article is licensed under a Creative Commons Attribution 4.0 International License, which permits the use, sharing, adaptation, distribution and reproduction in any medium or format, as long as appropriate credit to the original author(s) and the source is given by providing a link to the Creative Commons license and changes need to be indicated if there are any. The images or other third-party material in this article are included in the article's Creative Commons license, unless indicated otherwise in a credit line to the material. If material is not included in the article's Creative Commons license and your intended use is not permitted by statutory regulation or exceeds the permitted use, you will need to obtain permission directly from the copyright holder. To view a copy of this license, visit http://creativecommons.org/ licenses/by/4.0/.

©The Author(s) 2026.